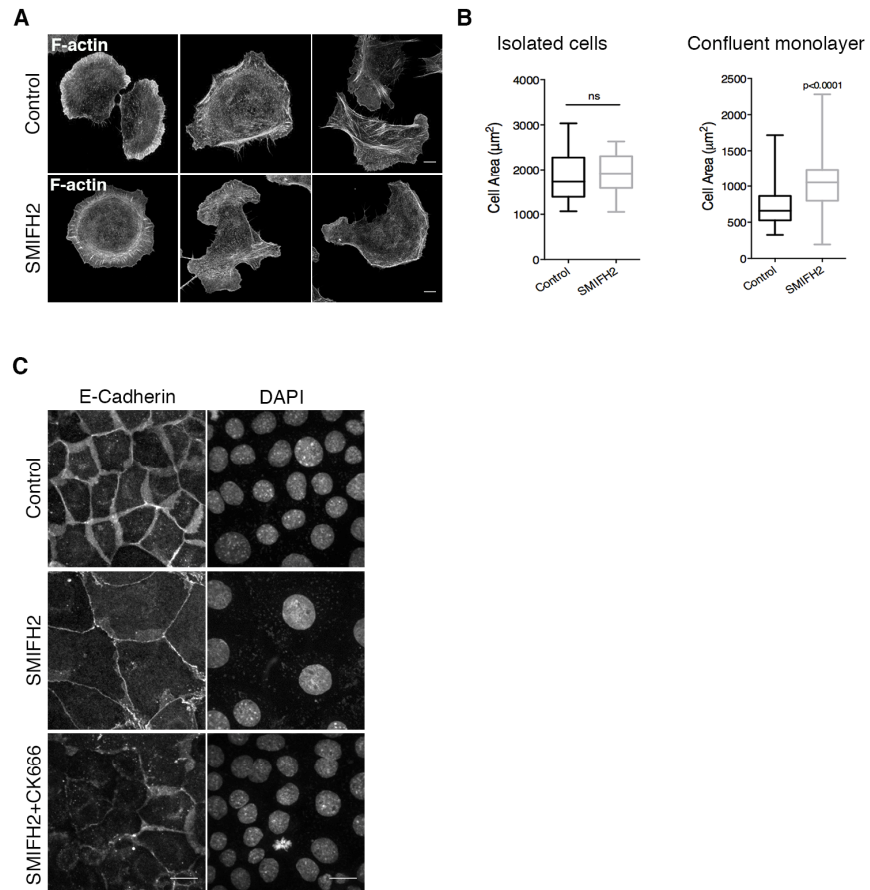


Supplemental Materials

Molecular Biology of the Cell

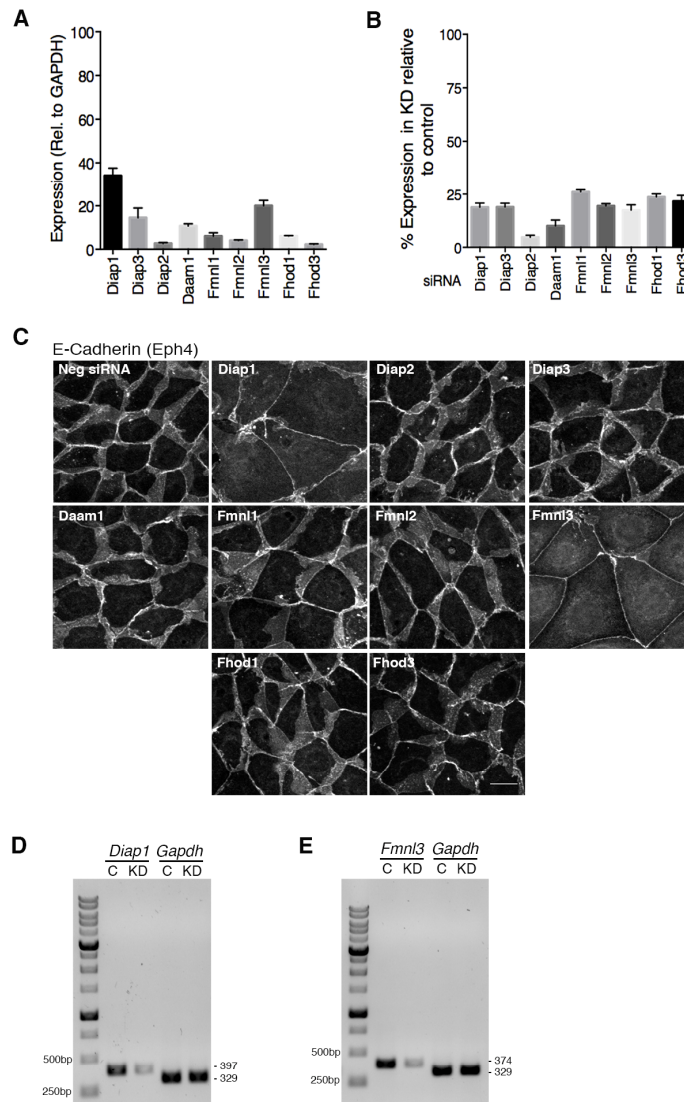
Rao et al.

SUPPLEMENTARY FIGURE LEGENDS



Supplementary Figure 1

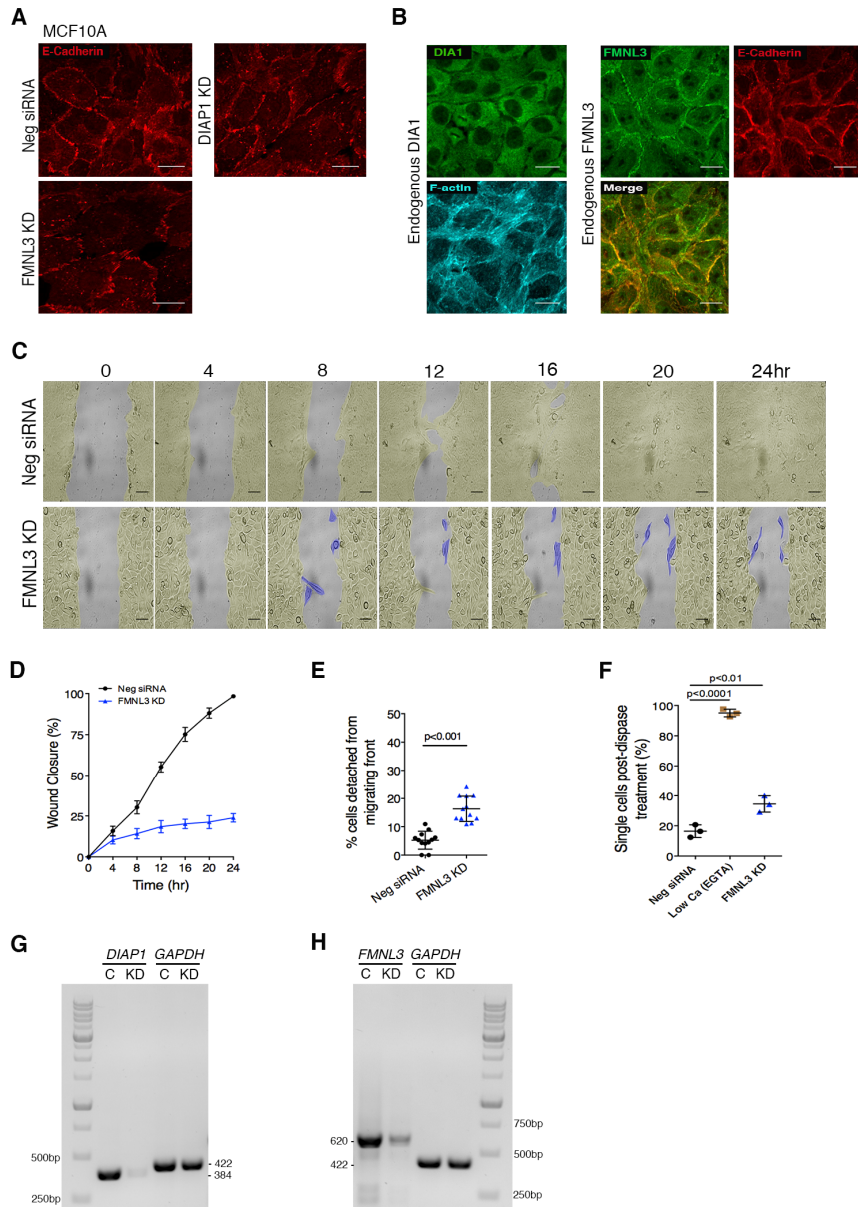
(A) Three examples each of isolated Eph4 cells in control and SMIFH2-treated conditions, labeled to visualize F-actin. (B) Quantification of cell area in isolated cells or confluent monolayers post-SMIFH2 treatment. Note that SMIFH2 treatment on isolated cells does not induce excess cell spreading. n=30 isolated cells or 100 cells in a monolayer. (C) Double inhibition of formin and Arp2/3 complex activities (SMIFH2+CK666, bottom panel) abrogates cell spreading induced by SMIFH2 (middle panel). Note the reduction in junctional E-cadherin with combined SMIFH2 and CK666 treatment (DAPI labeling shown for reference). Statistical significance assessed using Student's t-test in (B). Scale bars, 10 μ m (A); 20 μ m (C).



Supplementary Figure 2

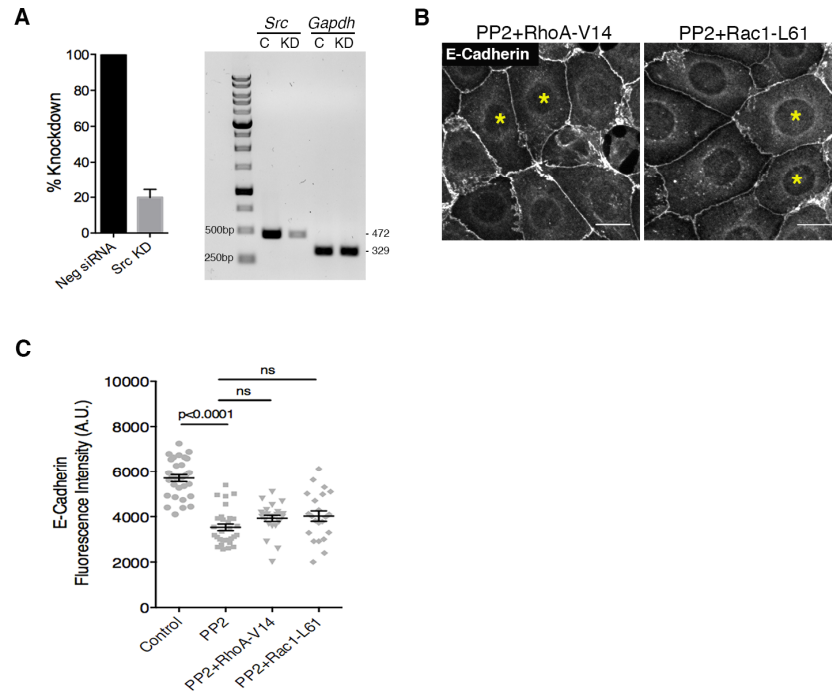
(A) Expression profile of Diaphanous-related family of formins in Eph4 cells. Error bars represent s.e.m., n=2 independent experiments. (B) Quantification of KD efficiency for Diaphanous-related family of formins. Error bars represent s.e.m., n=2-3 independent experiments. (C) Representative images of AJ morphology visualized by labeling E-cadherin after KD of individual formins as indicated. (D) & (E)

Representative gel images showing KD efficiency for formins *Diap1* and *Fmnl3* in Eph4, respectively. *Gapdh* was used as a control. C: Non-targeting control siRNA, KD: Knockdown. Scale bar, 20 μ m (C).



Supplementary Figure 3

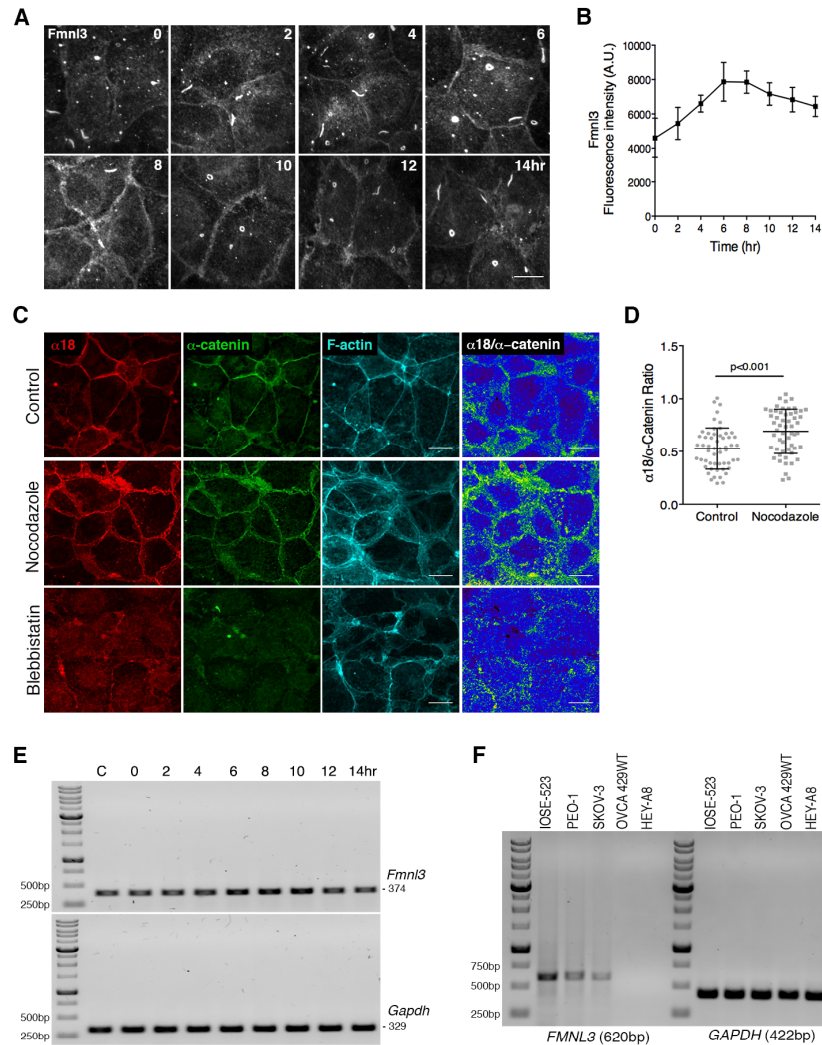
(A) Phenotypes obtained upon siRNA-mediated KD of DIAP1 or FMNL3 in MCF10A monolayers, labeled to visualize E-cadherin; note the reduction in lateral junctions and increased cell area associated with DIAP1 or FMNL3 KD. (B) Endogenous DIA1 exhibits diffuse localization in MCF10A cells (left panel), while endogenous FMNL3 localizes at the AJ (right panel), co-localizing with E-cadherin. (C) Montage from a movie of an *in vitro* scratch assay in control (Neg siRNA) or FMNL3KD conditions in MCF10A monolayers. Images are pseudo-colored in yellow to indicate cohesive regions of the cell sheet, and in blue (bottom panel) to highlight cells that have detached from the migrating front. Related to Supplementary Movie 5 and 6. (D) Quantification of wound closure. n=12 movies for each condition, with mean±s.e.m. (E) Quantification of cells detaching from migrating front (%). n=12 movies for each condition, with mean±s.d. (F) Dispase assay to determine adhesion strength in MCF10A for conditions tested in (C). EGTA treatment served as a low adhesion strength control. Individual dots represent a single experiment (n=3), with mean±s.d. (G) & (H) Representative gel images showing KD efficiency for formins *DIAP1* and *FMNL3* in MCF10A, respectively. *GAPDH* was used as a control. C: Non-targeting siRNA control, KD: Knockdown. Statistical significance assessed using Student's t-test in (E); one-way ANOVA in (F). Scale bars, 20µm (A and B); 50µm (C).



Supplementary Figure 4

(A) Quantification of KD efficiency for Src kinase. Error bar represents s.e.m., n=3 independent experiments. Representative gel image showing KD of *Src* is provided. *Gapdh* was used as a control. C: Non-targeting siRNA control, KD: Knockdown. (B) Expression of constitutively active RhoA-V14 or Rac1-L61 does not rescue Src inhibition phenotype (transfected cells marked with yellow asterisks). (C)

Quantification of E-cadherin intensity at the AJ for (B). Control cells were transfected with EGFP. n=25-30 cells from 3 experiments. Statistical significance assessed using one-way ANOVA in (C). Scale bar, 20 μ m (B).



Supplementary Figure 5

(A) Immuno-labeling for endogenous Fmnl3 during the process of wound closure over 14hr. Cells depicted here were located 4-5 cells rows behind the wound edge. Note the increased localization of Fmnl3 at the AJ between 6hr-10hr time points. (B) Quantification of Fmnl3 fluorescence intensity for (A). Error bars represent s.e.m., n=2 independent experiments. (C) Representative images of Eph4 monolayers labeled to visualize α -catenin α 18, α -catenin and F-actin following treatment with nocodazole or blebbistatin. α 18/ α -catenin ratio images illustrate the increase or decrease in force-dependent stretching of α -catenin at cell-cell junctions. (D) Quantification of α 18/ α -catenin intensity ratio for (C). n>50 junctions for each condition tested, with mean \pm s.e.m. (E) Uncropped gel image, related to Figure 6B. (F) Uncropped gel image, related to Figure 6F. Statistical significance assessed using Student's t-test in (D). Scale bars, 20 μ m (A and C).

Supplementary Table 1

ON-TARGET plus siRNA oligonucleotides used for gene knockdown

S.No	Gene Symbol	Species	Gene ID	Gene Accession	Sequence
1.	<i>Diap1</i>	Mouse	13367	NM_007858	AGGUCGGGCUUGCGGGAUA GGGAGAUGGUGUCGCAUA UCACACUGCUGGUCGAAA UGGAUGAGGUCGAACGCUU
2.	<i>Diap3</i>	Mouse	56419	NM_019670	CAUAAAUGCUCUCGUUACA GUGCAUUGUCGGCGAGGAA CAGGAUAGCGAAAGAGCGA GUGGAAGGCCUCCGGCAUA
3.	<i>Diap2</i>	Mouse	54004	NM_017398	CCGCAUGCCAUACGAGGAA GAUGAGAAAUACCGGGAUA GCAAUAUGUUGAAGCUCUA CCUAGAUGCUUGUGUAAAU
4.	<i>Daam1</i>	Mouse	208846	NM_172464	AGCGAAGAGUUGCGGGAUA CAGGAGAGGUGUUCGACAA GAUGAAAUCAAGCGGGCAA GCCCAAAGUAGAAGCGAUU
5.	<i>Fhod1</i>	Mouse	234686	NM_177699	CUACAUACCGUGAGCGCAA GUUUCGGACUUGUCGGGAA UCGCAUGAUUACCGAGACA UGAGAGUGCCCUUCGGUUA
6.	<i>Fhod3</i>	Mouse	225288	NM_175276	GGAACAAAUUAACCGGGA GCAGAGGAUAGAACGGGAA GAGCCGAGGCGGAUCAGAA CGGCAAGAGAGAGAGGAAA
7.	<i>Fmnl1</i>	Mouse	57778	NM_019679	GGGUUUAGGAGGCGAGUUC UUACACAGGUGCUGCGGGA AGAGAGAGUUUGUCGGCA CCUACAAGAAACGGGAACA
8.	<i>Fmnl2</i>	Mouse	71409	NM_172409.2	UGUUAUUGGUGCCGAAUA GGACUJAAAUGUGGACGAA CAAAGUCGACAGACGAAA GCGGAGAAAAGCAGCGUUU
9.	<i>Fmnl3</i>	Mouse	22379	NM_011711	GUAAGAACUGCAUCGGUU

					ACAACAGCGUCCUUCGAAA AGUUAUGAGCGUGAACGACA CCACUAAAAGUCCUACGGGA
10.	<i>Src</i>	Mouse	20779	NM_001025395	GCACGGGACAGACCGGUUA GGGAGCGGUGCAGAUUGU UCAGAUCGCUUCAGGCAUG GCUCGUGGCUUACUACUCC
11.	<i>DIAP1</i>	Human	1729	NM_005219.4	GAAGUGAACUGAUGCGUUU GAAGUUGUCUGUUGAAGAA GAUAUGAGAGUGCAACUAA GCGAGCAAGUGGAGAAUUAU
12.	<i>FMNL3</i>	Human	91010	NM_175736.4	AAGAACAGCUGGAGCGAUA CCUCAUUACUACGAGAGA AGGUAAGCUGCUGCGGCA GCAUGGUGGUCUUGGCUAU
13.	Neg siRNA	Mouse/ Human	-	-	UGGUUUACAUGUCGACUAA UGGUUUACAUGUUGUGUGA UGGUUUACAUGUUUUCUGA UGGUUUACAUGUUUUCUA

Supplementary Table 2

Gene-specific primers for semi-quantitative PCR analysis

S.No	Gene	Species	Forward Primer (5'-3')	Reverse Primer (5'-3')
1.	<i>Diap1</i>	Mouse	GGCCTAAATGGTCAAGGAGATAG	CAGAGGTGACAGCAGTGAAA
2.	<i>Diap3</i>	Mouse	GTGGACGATTTGGCACATTTAG	CTCTTTCTCTGCTCGCTCTTT
3.	<i>Diap2</i>	Mouse	CGCCATCTGAAGACAGGATAAT	CCGATAGGAGGAAGTGAAGAAAG
4.	<i>Daam1</i>	Mouse	CAGGCAGAGAAGATGAGGAAAG	GAACTCCTGCTGTCTTTGGTAG
5.	<i>Fhod1</i>	Mouse	TCTCCCTTCTGTCTCTCTATC	CCTTGGCTCTGGACTCAAATAG
6.	<i>Fhod3</i>	Mouse	GTTCTTCTCACACTCTCTTCC	GCGTCTCTCCATCTGACATAAA
7.	<i>Fmn1</i>	Mouse	CAGCCTATGTTTCCGACTT	GGGATGTGGTCTTGGGATTT
8.	<i>Fmn2</i>	Mouse	CCGTGTTCTCCCTGTCTTT	CTCGTCTGTAGGGTTGGTTTC
9.	<i>Fmn3</i>	Mouse	AAATACCCGGAAGTGGCTAAC	CGCATTACCTCTTGTCTTCT
10.	<i>Src</i>	Mouse	CTCGTGGCTTACTACTCAAAC	CATAGTTCATCCGCTCCACATAG
11.	<i>Gapdh</i>	Mouse	AACAGCAACTCCCACTCTTC	TGGGTGCAGCGAACTTTAT
12.	<i>DIAP1</i>	Human	CTCTCCTGGCTGTGTTATTT	CACCTCCCATTTCCTTGAGAC
13.	<i>FMNL3</i>	Human	CAAGAAGCAGGAGGAGTAATG	CTACAGACCTAGTCCCATAGT
14.	<i>GAPDH</i>	Human	GGTCGGAGTCAACGGATTT	TCTTGAGGCTGTTGTCATACTT